The impact of external environments and wheel-rail friction on noise inside a train car

Yoshiharu Soeta[a] and Ryota Shimokura[b]

[a]Health Research Institute, National Institute of Advanced Industrial Science and Technology (AIST), Midorigaoka, Ikeda, Osaka, 563-8577, Japan, E-mail: y.soeta@aist.go.jp

[b]Department of Otorhinolaryngology - Head and Neck Surgery Nara Medical University, Shijo-cyo, Kashihara, Nara, 634-8522, Japan, E-mail: rshimo@naramed-u.ac.jp

Trains travel through various environments typically on tracks above ground or in tunnels. When trains pass through different environments, the perceived noise inside a train car can change. For example, there are three main types of noise caused by wheel-rail interaction, namely, rolling, impact, and curve squeal. Each type can be perceived differently. To consider appropriate remedial measures, the effects of the external environment and wheel-rail interaction on noise inside train cars were investigated. Spectral analysis of noise from inside a train car traveling through tunnels featured a noticeable sound frequency around 250 Hz. More reflections enter train cars from tunnels with circular cross-section, namely those constructed by a boring machine. Impact noise had larger components at lower frequencies. Curve squeal noise had larger components at frequencies between 125 and 500 Hz.

1. INTRODUCTION

Railways are a major means of commuting and the average commute time is more than one hour in a typical metropolitan area of Japan. Consequently, workers and students spend long periods in train cars. The noise levels inside running train cars range from 60 to 100 dB for underground railways [1-4] and 60 to 80 dB for aboveground railways [5, 6]. The World Health Organization (WHO) has stated that the allowable duration of exposure to 85 dB (A-weighted noise) is approximately 45 min [7]. Some studies suggest that noise-induced hearing loss (NIHL) could be caused by cumulative daily short-term noise exposure of less than 85 dB [8-10]. Therefore, workers and students using railways on a daily basis are at risk of NIHL.

The characteristics of underground railway tunnels vary according to the excavation method. The cut-and-cover method (CCM) excavates a tunnel from ground level downwards, constructs the tunnel roof and sides, and buries the tunnel. Since the flat side walls and straight capping beams shape the configuration of tunnel, the cross-section of the tunnel is rectangular and relatively large (Fig. 1a). The boring machine method (BMM) drills tunnels using a boring machine and lines the inside with concrete, steel, or ductile iron segments. Since the boring machine has a circular cutter head at the front, the cross-section of the tunnel is circular and relatively small (Fig. 1b). The new Austrian tunneling method (NATM) excavates a tunnel that is maintained using retentive characteristics of the natural ground, the surface of which is quickly strengthened with shotcrete, and the insertion of reinforcing locking bolts. The characteristics of the sound fields in these three tunnel types are more than likely to differ.

It has been shown that the noise level inside underground train cars is higher than that inside above-ground train cars [2, 4], because of reflections from the tunnel walls. Train noise, such as the noise of rolling wheels and the engine, for above-ground railways is emitted outside the train and does not reflect back into the train car, while train noise for underground railways is also emitted outside the train, but is reflected off tunnel walls back into the train car. Therefore, the sound

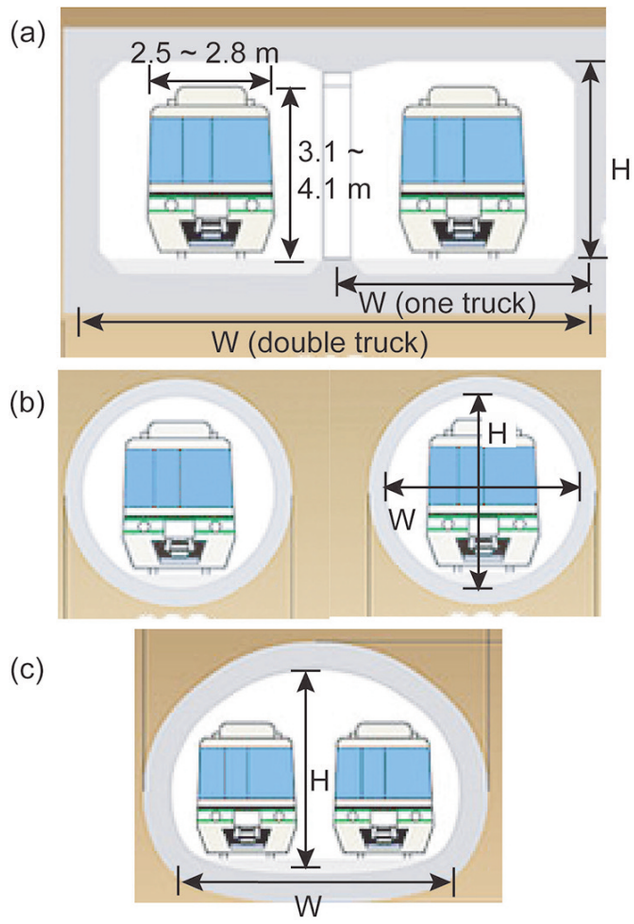

Figure 1. Cross-sections of (a) CCM, (b) BMM, and (c) NATM tunnels.

environment inside the train car is determined not only by the train noise, but also by the outside environment.

People hear some types of noise in train cars. Researchers have studied mechanisms for generating different types of noise such as rolling, impact, curve squeal [11-15], motor (fans), [16, 17], aerodynamic noises [18, 19]. Some studies have modeled the noise in train cars to help predict and reduce it [20-23]. Although some studies have quantitatively [1-3, 18-21] [1, 2, 5, 6, 24, 25] and qualitatively [6, 24] investigated the noise characteristics inside running train cars, the effects of noise sources on the noise characteristics have not been evaluated qualitatively. This should be clarified to improve the acoustical environment in a train car for the passenger.

The aim of this study was to clarify the characteristics of noise inside train cars. In particular, this work focuses on the effects of the outside environment, either above-ground or underground environment, the cross-section of tunnels, and noise sources from rolling, impact, and curve squeal noises on noise inside train cars. The acoustic treatment (i.e., sound absorption, insulation, and active noise control) of tunnels is an effective solution for improving the sound environment inside train cars. To consider an appropriate acoustic treatment, it is necessary to clarify the characteristics of the noise inside train cars. Two types of measurements were conducted: an impulse response measurement for evaluating the characteristics of sound fields in CCM and BMM tunnels; and, noise

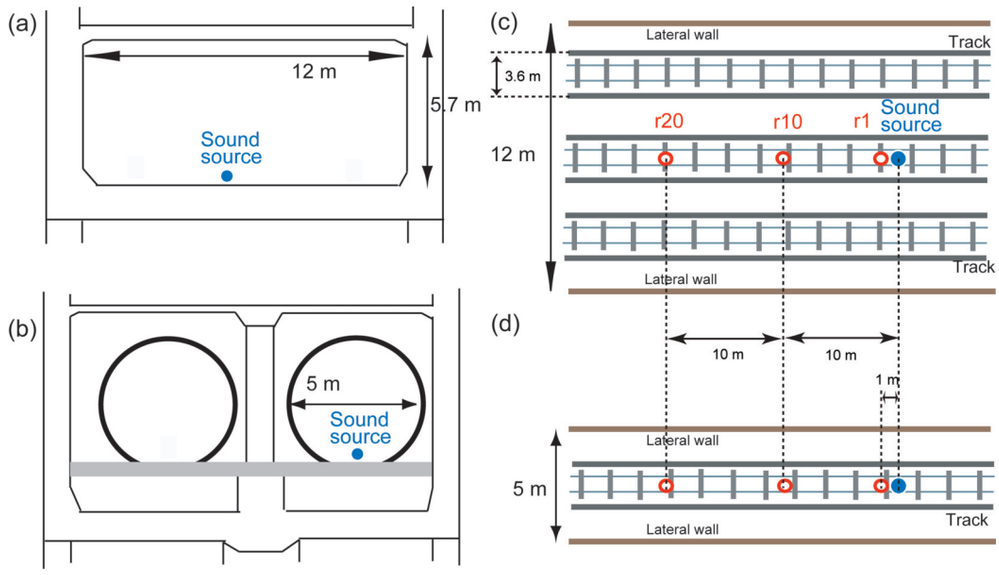

Fig. 2. Soeta and Shimokura

Figure 2. Cross-sectional and planar views of the sound source and microphone (r1, r10, and r20) positions for the impulse response measurement in (a, c) CCM and (b, d) BMM tunnels.

measurements taken inside a running train car to evaluate the effects of the outside environment and noise sources.

2. METHOD

2.1. IMPULSE RESPONSE MEASUREMENT

Impulse responses were measured in CCM and BMM tunnels. CCM and BMM tunnels were covered by concrete and ductile iron segments, respectively. It was difficult to measure the impulse responses in an NATM tunnel for safety reasons. There were no trains in the tunnel. The sound source was an omni-directional loudspeaker (Type 4292, B&K). It was placed (without a tripod stand) directly on the railway track in the tunnel (Fig. 2) since the most important noise inside a train is generated at the wheel-rail contact [14]. A binaural microphone (Type 4101, B&K), which was located at the ears of a standing experimenter (1.6 m), was used to record the impulse responses. The experimenter always faced the sound source. The microphone was located at 1, 10, and 20 m from the sound source (r1, r10, and r20).

A sinusoidal signal with an exponentially-varying frequency sweeping from 40 Hz to 20 kHz over a period of 18 s was used. A personal computer (Let's Note, Panasonic) generated the signals and recorded the responses via the binaural microphone and an AD/DA converter (AudioFire8, Echo Digital Audio) at a sampling rate of 48 kHz and sampling resolution of 24 bits. The recorded responses were deconvolved so that the impulse responses could be obtained [25].

Acoustic parameters (i.e., strength (G), reverberation time (RT), and interaural cross-correlation coefficient (IACC)) were calculated [26] from the impulse responses at the left and right ear positions, i.e., $p_l(t)$ and $p_r(t)$. G is the logarithmic ratio of the measured sound pressure to the sound pressure that would be measured at a distance of 10 m from the same sound source in a free sound field, and is given by

$$IACC = \left| \frac{\int_0^\infty p_l(t)p_r(t-\tau)\,dt}{\sqrt{\int_0^\infty p_l^2(t)\,dt \int_0^\infty p_r^2(t)\,dt}} \right|_{\max} \quad |\tau| \le 1\,[ms], \tag{1}$$

where p(t) is the sound pressure measured at the left, pl(t), or the right, pr(t), ear position, and p10(t) is that measured at a distance of 10 m in an anechoic room, employing the same measurement chain and the same settings used during the on site survey. RT is the time required for the sound pressure level to decrease by 60 dB, at a rate of decay given by the linear least-squares regression of the measured decay curve from a level of 5 dB below the initial level to 35 dB below the initial level. The IACC is defined as the maximum correlation of the sounds arriving at the left and right ears, and is given by .

$$IACC = \left| \frac{\int_0^\infty p_l(t)p_r(t-\tau)\,dt}{\sqrt{\int_0^\infty p_l^2(t)\,dt \int_0^\infty p_r^2(t)\,dt}} \right|_{\max} \quad |\tau| \le 1\,[ms], \tag{2}$$

where τ is the delay time

Table 1. Dimensions of tunnels

Tunnel	Width [m]	Height [m]
CCM (single track)	4.2	5.3
CCM (double track)	7.8 – 9.1	4.2 – 5.3
BMM	4.2 – 5.7	4.2 – 5.7
NATM	7.7 – 8.7	5.8 – 6.5

2.2. NOISE MEASUREMENT

Noise was measured continually in a train car traveling from one terminal station to another terminal station on 10 lines. Different types of train car run on each line. Intervals between stations were selected for analysis according to the outside environment of the train car; that is, CCM (single and double tracks), BMM, and NATM tunnels, and the above-ground environment. The numbers of intervals in which measurements were made were 4, 15, 13, 5, and 20 for the CCM (single track), CCM (double track), BMM, and NATM tunnels, and above ground respectively. The cross-sectional area of each tunnel is given in Table 1. All tunnels were covered by concrete except for a small part of the BMM tunnels, which was covered by steel segments. Trains run on a slab track in the tunnels and on a ballast track above ground.

The three types of noise caused by wheel-rail interaction are rolling, impact, and curve squeal. The rolling type was defined as noise in running train cars that include no impact or curve squeal noise. We listened to the recorded sound to identify the impact and curve squeal noise. This noise was cut out from the data, and the durations were at least 10 s. It was difficult to determine beforehand that measurement was carried out in motor or trailer cars because some types of trains usually run on the line. Thus, data from motor and trailer cars were mixed.

A dummy-head microphone (KU100, Neumann) and a surround microphone (MKV, SoundField) were used to record noise inside a train car. The dummy head is an artificial model of the human head with two microphones inserted at the entrances of the outer ears. The surround microphone is composed of four closely spaced subcardioid microphone capsules based on a virtual single point. The recorded signal can be separated into signals coming from three dimensions (X: front-back, Y: left-right, Z: up-down) and an omni-directional signal (W) originating from the same central point. The microphones were located in the area for a wheelchair user. The microphones always faced the inside of the train cars and were perpendicular to the direction of travel. The heights of the dummy head and surround microphones were 1.6 m and 1.3 m respectively. For all measurements, noise was recorded on a personal computer (Let's Note, Panasonic) via an AD/DA converter (AudioFire8, Echo Digital Audio) at a

sampling rate of 48 kHz and sampling resolution of 24 bits. The measurements were carried out from 10:00 to 15:00 to avoid rush-hours commuting.

To evaluate the noise inside train cars, the octave-band power levels, the A-weighted equivalent continuous sound pressure level (L_{Aeq}), and parameters extracted from interaural cross-correlation/autocorrelation functions (IACF/ACF), were derived from the left and right output signals $p_l(t)$ and $p_r(t)$ from the dummy-head microphones. L_{Aeq} is widely used for the measurement of noise inside train cars [27]. The octave-band power levels and L_{Aeq} were determined from the time-averaged sound pressure levels of the octave-band filtered and A-weighted pl(t) and pr(t).

The IACF/ACF parameters of noise are proposed for describing the sound quality [28]. The normalized IACF for the signals received at each ear, $p_l(t)$ and $p_r(t)$, as a function of the running step, s, is defined by

$$\phi_{lr}(\tau) = \phi_{lr}(\tau, s, T) = \frac{\Phi_{lr}(\tau; s, T)}{\sqrt{\Phi_{ll}(0; s, T)\Phi_{rr}(0; s+\tau, T)}} \tag{3}$$

where

$$\Phi_{lr}(\tau; s, T) = \frac{1}{2T}\int_{s-T}^{s+T} p_l'(t)p_r'(t+\tau)dt \tag{4}$$

Here $\Phi_{ll}(0)$ and $\Phi_{rr}(0)$ are the ACFs at $\tau = 0$ for the left and right ears, $2T$ is the integration interval, and $p'_{l,r}(t) = p_{l,r}(t) \star s(t)$, $s(t)$ being the ear sensitivity. For convenience, $s(t)$ was chosen as the impulse response of an A-weighted network, which includes the transfer function of the human outer and middle ear [28, 29]. The IACC is defined as the maximum correlation of the sounds arriving at the left and right ears, and is related to the subjective diffuseness and ASW [30-32]. The IACC is given by

$$\mathrm{IACC}(s, T) = \left|\phi_{lr}(\tau, s, T)\right|_{\max}, |\tau| \le 1\ [\mathrm{ms}]. \tag{5}$$

In a similar way, the normalized ACF of a signal received at an ear, $p_l(t)$ or $p_r(t)$, can be obtained by substituting $p'_l(t)$ ($p'_r(t)$) for $p'_r(t)$ ($p'_l(t)$) in Eq. (4). The ACF parameters, τ_1 and ϕ^1, are defined as the time delay and the amplitude of the first maximum peak and are related to the perceived pitch and pitch strength (i.e., tonality) of the complex sounds [29, 33]. The other ACF parameter, $W_{\Phi(0)}$, is defined as the width of the first decay and corresponds to the spectral centroid [6, 29].To identify pathways and proportions of the dominant noise, the direction of arrival (DOA) and energy proportions were derived from the output signals $p_w(t)$, $p_x(t)$, $p_y(t)$, and $p_z(t)$ of the surround microphone. The omni-directional signal, $p_w(t)$, is proportional to the sound pressure, $p(t)$, at the measurement position. The orthogonal figure-of-eight signals, $p_x(t)$, $p_y(t)$, and $p_z(t)$, are proportional to the component of the particle velocity in the corresponding direction. Instantaneous intensities in the three directions can be calculated using the product of the instantaneous sound pressure, $p_w(t)$, and the orthogonal figure-of-eight signals, $p_x(t)$, $p_y(t)$, and $p_z(t)$ [34]. By applying a short-time Fourier transform, the frequency distribution of intensity in the front-back direction was defined by,

$$I_x(\omega; t, T) = \frac{\sqrt{2}}{Z_0}\mathrm{Re}\left\{p_w^*(\omega; t, T)p_x(\omega; t, T)\right\} \tag{6}$$

where Z_0 is the acoustic impedance of air, T is the time window, and $\star$ denotes the complex conjugate [35]. The sound intensities in the other two directions, I_y and I_z, can be given in a similar manner. The azimuth and the elevation angles were obtained using the vector sum of the active intensities I_x, I_y, and I_z,:

$$Azimuth(\omega;t,T) = \tan^{-1}\left[\frac{-I_y(\omega;t,T)}{-I_x(\omega;t,T)}\right] \quad (7)$$

$$Elevation(\omega;t,T) = \tan^{-1}\left[\frac{-I_z(\omega;t,T)}{\sqrt{I_x^2(\omega;t,T)+I_y^2(\omega;t,T)}}\right] \quad (8)$$

The azimuth and elevation angles were calculated for the time window of 0.5 s.

The IACC, τ_1, ϕ_1, and $W_{\Phi(0)}$ were calculated for every given time window or integration interval $2T$. The start of each analysis was delayed for a short time, which is the running step. The moving analysis aids in the effective description of the temporal change in the parameters. In this study, the time window or integration interval, $2T$, was 0.5 s, and the running step was 0.1 s.

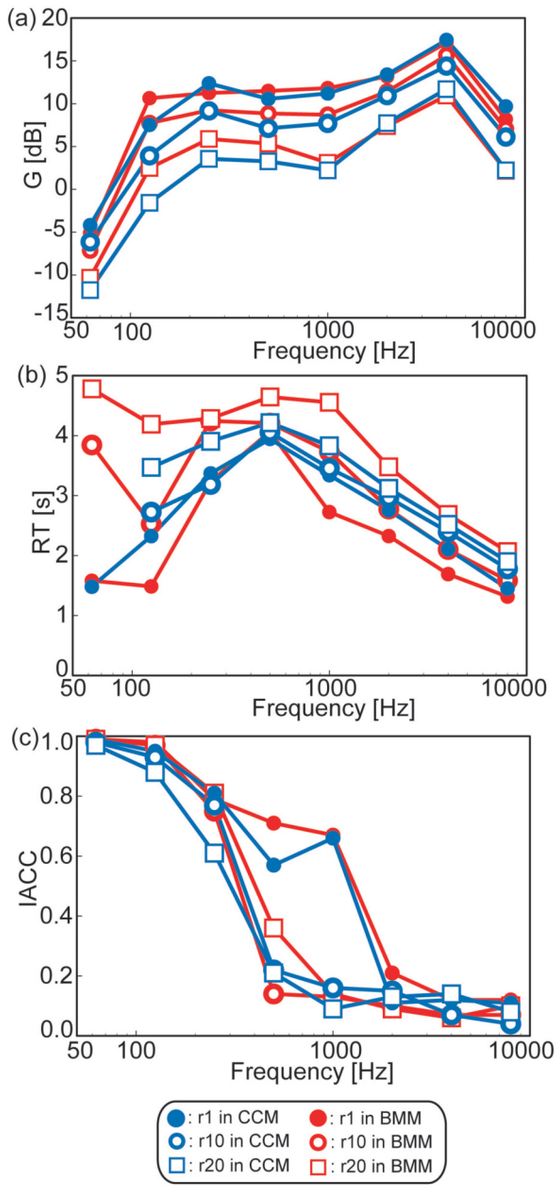

Figure 3. *(a) G, (b) RT, and (c) IACC as functions of the 1/1 octave band centre frequency in the CCM and BMM tunnels. The symbols indicate the locations of the microphones in CCM and BMM tunnels, respectively.*

2.3. SUBJECTIVE ANNOYANCE TEST

Eight stimuli were selected from noise in running train cars. The stimuli were presented binaurally through headphones (HD650, Sennheiser). Eight subjects aged 20 to 47 years with no history of hearing disorders participated in the experiment. They sat in a comfortable thermal environment in a soundproof room and heard the sound stimuli. Paired-comparison tests were performed for all combinations of pairs (i.e., 28 pairs (N(N–1)/2, N = 8)) of stimuli, interchanging the order that the stimuli in each pair were presented in each session and presenting the pairs in random order. Six sessions were conducted for each subject. The duration of the stimuli was 5.0 s, the rise and fall times were 100 ms, and the silent interval between stimuli was 1.0 s. After the presentation of the two stimuli, subjects were asked to judge which of the two sound signals was more annoying. The scale values of the annoyance were calculated according to Case V of Thurstone's theory [36].

3. RESULTS AND DISCUSSION

3.1. SOUND FIELD MEASUREMENT

Figure 3 presents the acoustic parameters calculated from the impulse responses in the CCM and BMM tunnels. The G values around 125, 500, and 1000 Hz in the BMM tunnel were higher than those in the CCM tunnel. The G values at a position far from the noise source, r20, at lower frequencies (63-500 Hz) were higher in the BMM tunnel, suggesting the smaller circular cross-section had a focusing effect. RT had a peak at around 500 Hz for both tunnels. RT values at low and middle frequencies at a position far from the noise source, r10 and r20, were longer in the BMM tunnel as shown in Fig. 4, suggesting an increase in the noise level due to reverberation in the BMM tunnel. The values of IACC at frequencies lower than 1000 Hz in the CCM tunnel were larger than those in the BMM tunnel at r20. This suggests an increase in diffuseness due to complex reflections in the rectangular cross-section of the CCM.

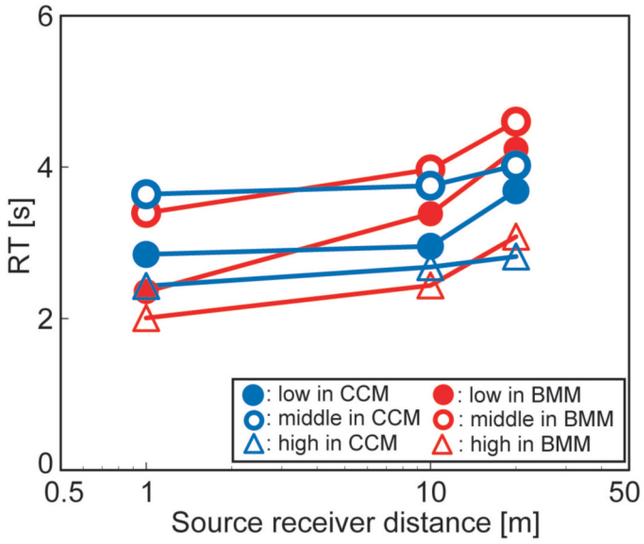

Figure 4. RT as a function of the source-receiver distance at low (125 and 250 Hz), middle (500 and 1000 Hz), and high (2000 and 4000 Hz) frequencies in CCM and BMM tunnels, respectively.

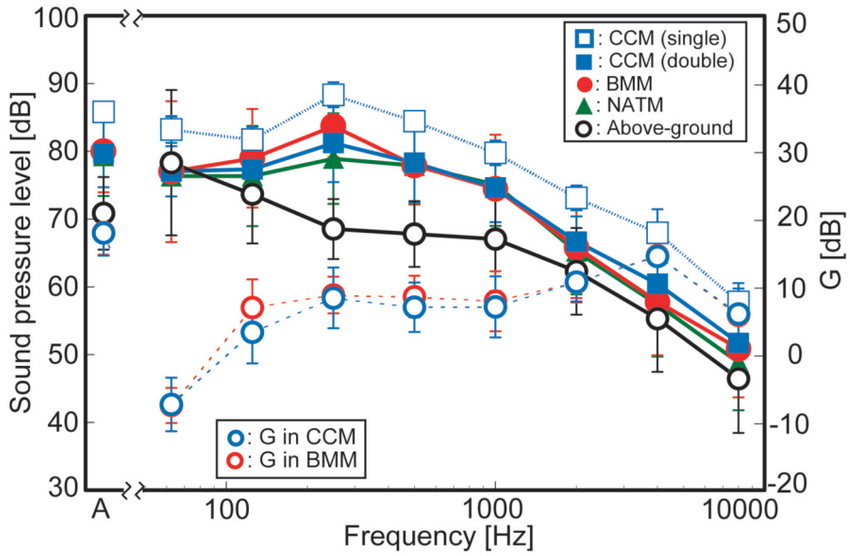

Figure 5. Measured sound pressure level as a function of the 1/1 octave band centre frequency and LAeq in CCM (single track), CCM (double track), BMM, NATM tunnels, and above-ground. The averaged G values for r1, r10, and r20 in sound field measurements are indicated for CCM (triple track) and BMM tunnels for comparison.

3.2 NOISE MEASUREMENT

Figure 5 shows the L_{Aeq} and octave-band power levels. The L_{Aeq} in the tunnels was 8 to 15 dB higher than that above ground. Trains usually run on tracks mounted on concrete slabs in the tunnels and on ballasted track above ground. Tracks mounted on concrete slabs are generally found to be noisier than ballasted tracks, typically by 3 to 5 dB [14, 37], suggesting that the reflections in the tunnels increased L_{Aeq} by 3 to 12 dB. In all types of tunnel, the power level had a peak around 250 Hz. In contrast, the power level dipped around 250 Hz above ground. The difference between the power levels in tunnels and above-ground was large in frequency bands around 250 and 500 Hz. These results suggest the effect of reflections in tunnels can be mainly observed around 250 and 500 Hz and the source could be rolling, locomotive exhaust, and cooling fan noise [13, 17, 36-39]. When a train enters a tunnel, the major frequency component shifts from lower to higher frequency ranges [10], agreeing with the present results. The sectional area of the CCM tunnel has clear effects on noise levels. The smaller CCM tunnels had larger noise levels

In comparison with octave-band power levels of the sound field and noise measurements as shown in Fig. 5, noise emitted from the train car is observed at frequencies higher than 2000 Hz. The averaged G values of r1, r10, and r20 for triple-track CCM and BMM tunnels were nearly identical. It is assumed that the octave-band power levels in the BMM tunnel were smaller than those in the single- and double-track CCM tunnels since the smaller CCM tunnels had higher noise levels in the noise measurement. This was not the case and suggests that the longer RT at a location far from the noise source was responsible for the increase in the noise level in the BMM tunnels. To reduce such effects, a concave surface for the BMM tunnels might be useful for resonance-type sound absorption or reducing cooling fan noise [40] and active noise control [41] might be useful for noise reduction at the source.

On the basis of a running analysis, the frequency distributions of the IACC, τ_1, ϕ_1, and $W_{\Phi(0)}$ for each outside

environment were obtained (Fig. 6). The IACC was largest for the BMM tunnel, smaller for the CCM and NATM tunnels, and smallest above ground. This agrees with the results of sound field measurements, which shows that the IACC at lower frequencies for the CCM tunnel was larger than that for the BMM tunnel at r20. More reflections were evident inside the train cars in the BMM tunnels because of the circular cross-section. In contrast, fewer reflections were evident inside the train cars in the NATM tunnels because of the complex cross-section. The values of τ_1 were concentrated at 1 ms, which corresponds to a frequency of 1000 Hz, for the NATM tunnel and above ground. The noise at 1000 Hz could be rolling noise emitted from the wheels and rails [13, 37], locomotive exhaust and cooling fan noise [17, 38-41]. The values of τ_1 were concentrated at 4 and 5 ms, which corresponds to a frequency of

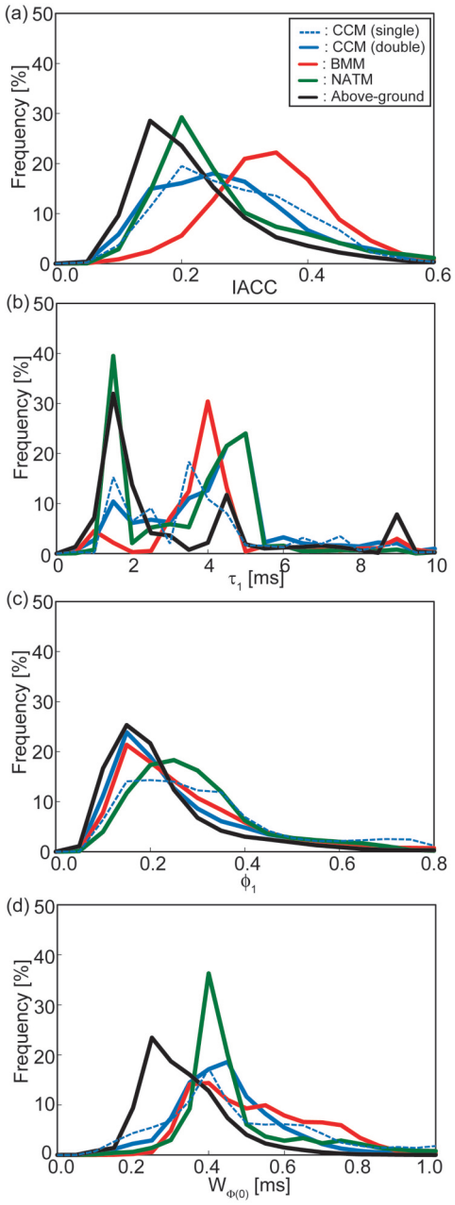

Figure 6 *Frequencies distributions of (a) IACC, (b) 1, (c) 1, and (d) W (0) obtained from short-time moving analyses for each outside environment.*

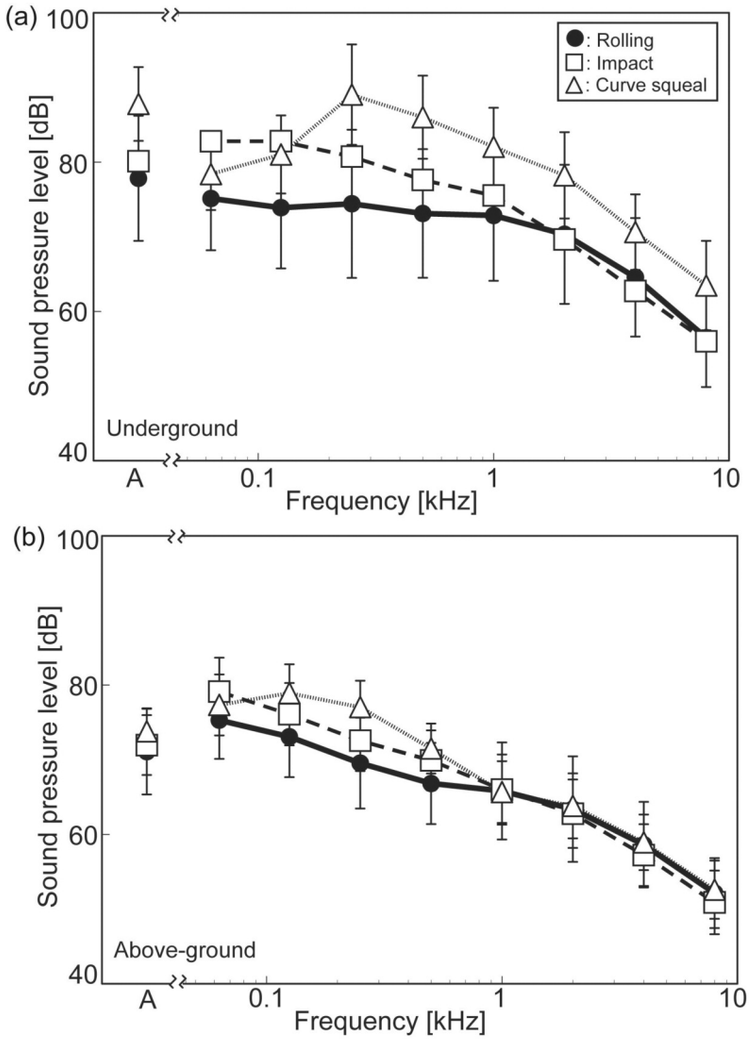

Figure 7. Measured sound pressure level as a function of the 1/1 octave band centre frequency and LAeq in (a) underground and (b) above-ground trains.

250 and 200 Hz, for the CCM, BMM, and NATM tunnels. The frequency of 250 Hz corresponded to the dominant frequency component in the BMM tunnel (Fig. 3a). The noise at 200 and 250 Hz could be locomotive exhaust and cooling fan noise [17, 38]. ϕ_1 was largest for the NATM tunnel, smaller for the BMM and CCM tunnels, and smallest for above ground. The reflections in tunnels could increase ϕ_1, and the perceived pitch strength of noise inside the train cars might be stronger in tunnels and cause more annoyance [42, 43]. $W_{\Phi(0)}$ was largest for the BMM tunnel, smaller for CCM and NATM tunnels, and smallest for above-ground. This suggests that the tunnel lowers the spectral centroid of noise inside the train cars. The sectional area of the CCM tunnel has no clear effect on IACF and ACF parameters.

Figure 7 shows the averaged LAeq and octave band levels for rolling, impact, and curve squeal noise in running above-ground and underground trains. Impact noise had larger components at lower frequencies (less than 500 Hz) compared to rolling noise in both underground and above-ground trains. Curve squeal noise had larger components at frequencies higher than 125 Hz in underground trains and at frequencies between 125 and 500 Hz s in above-ground trains compared to rolling noise. Underground trains often

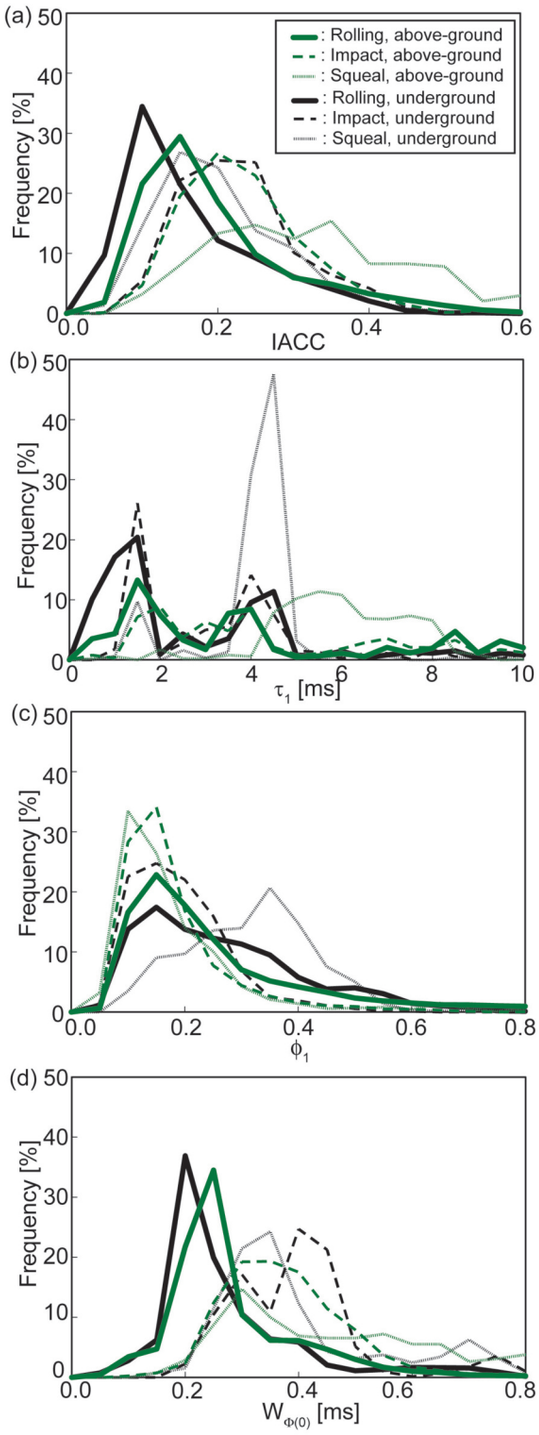

Figure 8. Frequencies distributions of (a) IACC, (b) 1, (c) 1, and (d) W (0) obtained from short-time moving analyses for each noise source.

run sharp curves because of geographical constraints, while above-ground trains rarely run sharp curves. This might affect the difference in higher-frequency components in underground and above-ground trains.

Figures 8 show the frequency distributions of the IACC, τ_1, ϕ_1, and $W_{\Phi(0)}$ for rolling, impact, and curve squeal noise in above-ground and underground trains. The τ_1 values concentrated around 1.5 and 4.0 ms.

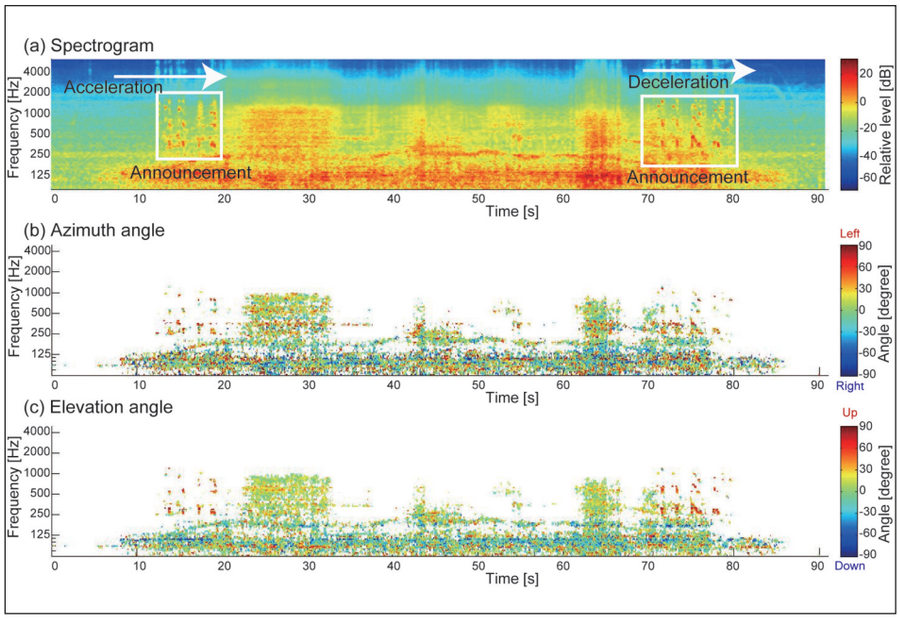

Figure 9. *(a) Spectrogram, (b) azimuth, and (c) elevation angle as a function of time for a CCM (double track) tunnel.*

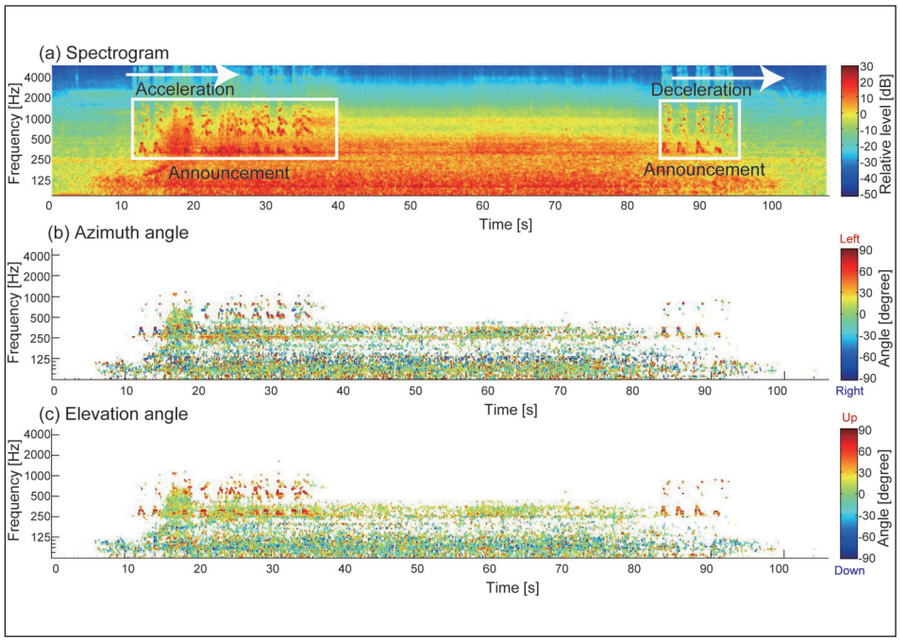

Figure 10. *(a) Spectrogram, (b) azimuth, and (c) elevation angle as a function of time for a BBM tunnel.*

Curve squeal noise had longer τ_1 values compared to rolling and impact noise in both above-ground and underground trains. Curve squeal noise had the largest ϕ_1 values in underground trains, suggesting the effect of both wheel-rail friction and reflections in tunnels. Impact and curve squeal noise showed the larger $W_{\Phi(0)}$ and IACC values compared to rolling noise in both above-ground and underground trains, suggesting an increase in lower-

frequency components and binaural coherence. An increase in binaural coherence may cause higher annoyance [44].

Figures 9 and 10 show the spectrogram and DOA of the noise inside a train car in the CCM (double track) and BMM tunnels. The spectrogram was calculated from the omni-directional signal, $p_w(t)$. Red and blue areas indicate that the noise comes from the left and right, respectively, in

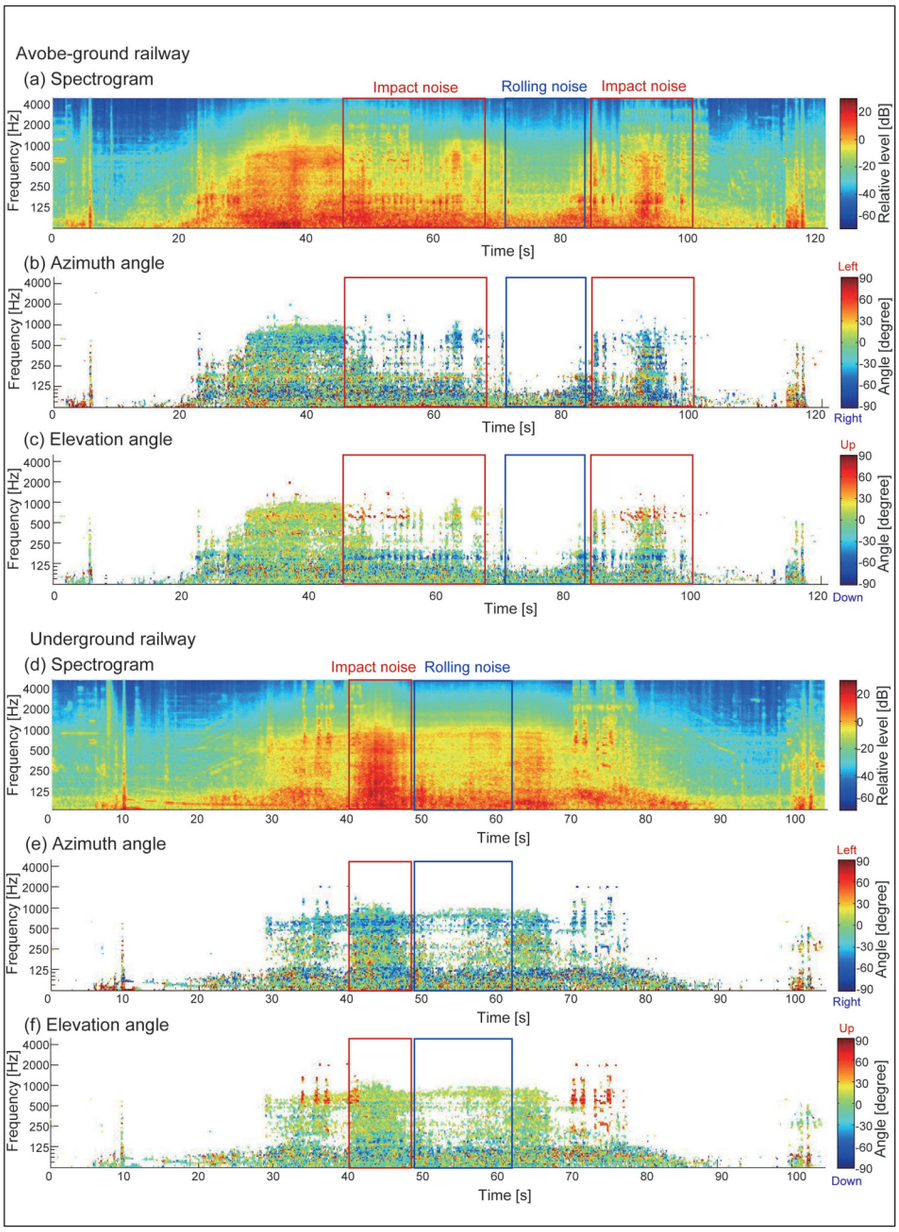

Figure 11 (a) Spectrogram, (b) azimuth, and (c) elevation angle as a function of time for rolling and impact noise.

Table 2. Correlation between the annoyance scale and ACF/IACF parameters

	L_{Aeq}	ø1	Wø(0)	I_{ACC}
Correlation coefficients	0.72	0.38	-0.15	-0.48

*P < 0.05

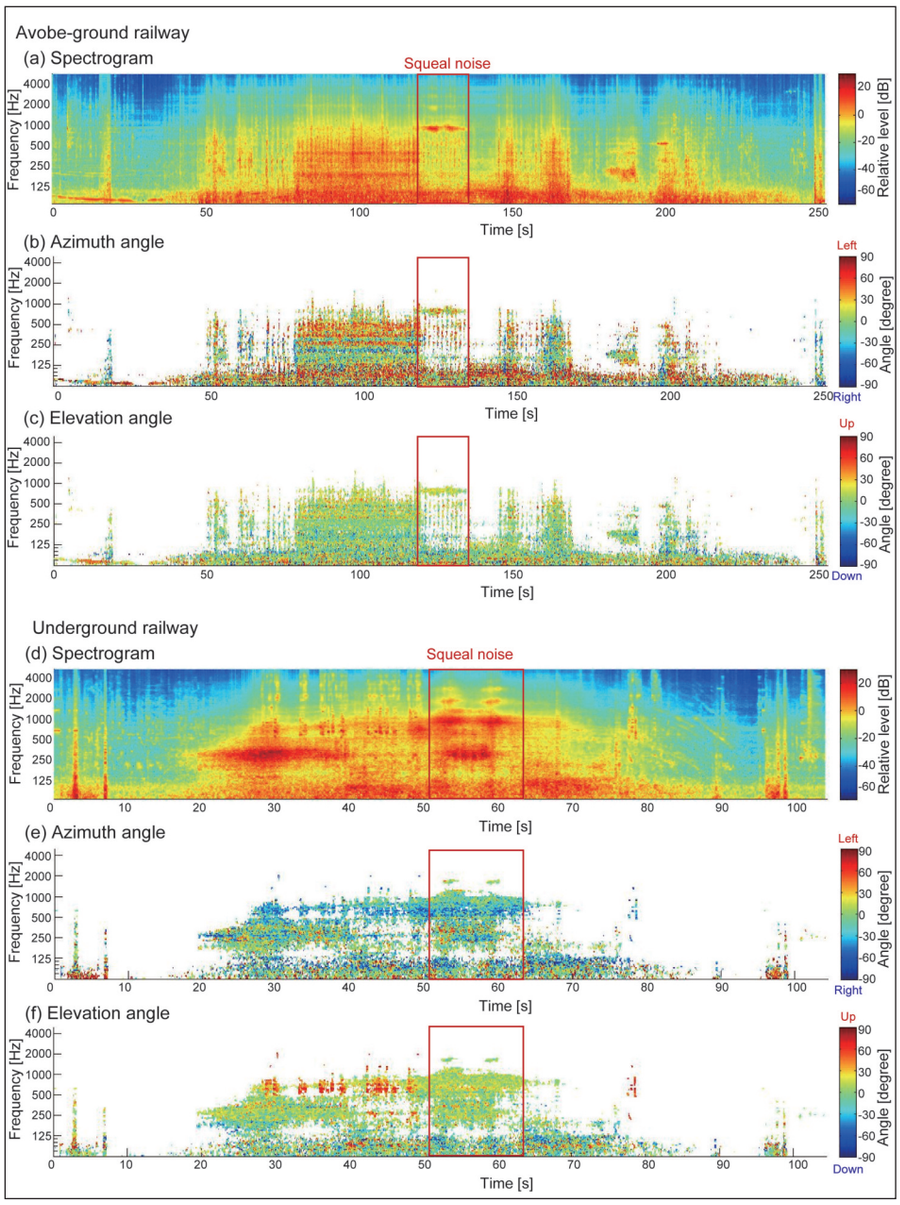

Figure 12 *(a) Spectrogram, (b) azimuth, and (c) elevation angle as a function of time for a curve squeal noise.*

Table 3. Standardized regression coefficients for the ACF/IACF parameters.

	a_1	a_2	a_3	a_4
Standardized coefficients	0.47**	0.15	-0.01	-0.40*

**$P < 0.01$, *$P < 0.05$

Figs 9b and 10b, and from above and below, respectively, in Figs 9c and 10c.

In the CCM tunnel, when the train ran (15–95 s), the noise component was concentrated in a frequency band around below 125 Hz (Fig. 9a) and the component came from below, and could thus be generated by locomotive exhaust noise [38, 39] (Fig. 3c). The noise component could be due to both structure-borne propagation, which is vibration propagating through the body of the train car and radiating into the internal cavity by the floor, and airborne

propagation due to the lack of insulation at those frequencies. Announcements by the public address (PA) system were observed (20–30 s and 80–90 s), and they came from above because the PA system was located in the ceiling of the train car (Fig. 9c).

In the BMM tunnel, when the train ran (25–110 s), the noise component was concentrated not only in a frequency band below 125 Hz, but also in a frequency around 250 Hz (Fig. 10a). The noise component in the frequency band around 125 Hz could be the solid-borne noise propagating from the floor (Fig. 10c). The noise component in the frequency band around 250 Hz came obliquely from above (Fig. 10c), and could be air-borne noise transmitting through the windows and doors of the train car. Since the cross-section of the BMM tunnel is circular and smaller than that of the CCM tunnel, some resonance may occur in the BMM tunnel. Announcements by the PA system came (30–50 s and 100–110 s) came from above (Fig. 10c).

Figures 11 and 12 show the spectrogram and DOA of rolling, impact, and curve squeal noise. The rolling noise was concentrated in a frequency band below around 125 Hz and the component came from below (Fig. 11). The impact noise had wider frequency components. The low frequency components below 125 Hz came from below and the high frequency components came from obliquely above or below (Fig. 11). The curve squeal noise was observed in the frequency band below 1000 Hz, directed from obliquely above (Fig. 12). Such noise could be air-borne noise transmitted through the windows and doors of the train car.

3.3. SUBJECTIVE ANNOYANCE TEST

The correlations between the annoyance and ACF/IACF parameters are listed in Table 2. Since τ_1 values were not normally distributed, they were ruled out of the correlation analysis. The contribution of each parameter to annoyance was investigated in multiple regression analysis. Four ACF/IACF parameters were examined:

$$\text{Annoyance} \approx a1L_{Aeq} + a_2\ 1 + a_{3W}\ (0) + a_{4IACC} + c. \quad (9)$$

The standardized partial regression coefficients in Eq. 9 are listed in Table 3. The regression coefficient was 0.76. L_{Aeq} and IACC were significant factors in the prediction of annoyance. L_{Aeq} has the greatest effect on subjective annoyance. Perceived annoyance increased with increasing L_{Aeq} and decreasing IACC. Negative correlation between annoyance and the IACC suggests that reflections from many directions may cause greater annoyance. This is consistent with previous findings on the annoyance of noise in train stations [45] and heavy-weight floor impact sounds [46].

4. CONCLUSION

To clarify the impact of the external environment and noise sources on noise inside a train car, experimental measurements were made of the sound field and noise. The sound fields were evaluated using G, RT, and the IACC calculated from impulse responses. The noise inside the train car was evaluated using the octave-band power levels, L_{Aeq}, IACC, τ_1, ϕ_1, and $W_{\Phi(0)}$. The results indicate that the noise inside train cars traveling through the tunnels included a prominent sound energy around 250 Hz and the reflections in the tunnels increased LAeq by 3 to 12 dB, with sound coming from the direction of the doors and windows of the train car. This suggested the effectiveness of the acoustic treatment in the side walls for the low frequency band. The geometry of the tunnel affected the RT and IACC. The

RT at low and middle frequencies far from the noise source was longer for BMM tunnels; also, the IACC was largest for BMM tunnels. More reflections seem to enter train cars in BMM tunnels because of their circular cross-section. The dimensions of the tunnel affected the noise level, with smaller CCM tunnels having larger noise levels. Impact noise had larger components at lower frequencies (less than 500 Hz) compared to rolling noise. Curve squeal noise had larger components at frequencies above 125 Hz in underground trains and at frequencies between 125 and 500 Hz in above-ground trains compared to rolling noise. Curve squeal noise had longer τ_1 values compared to rolling and impact noise. Perceived annoyance increased with increasing L_{Aeq} and with decreasing IACC. This suggests that reflections from many directions may cause higher annoyance.

Technological advances in designing trains and tracks (e.g., wheel absorbers, damping devices, variable-frequency drives and long rails without joints) have reduced train noise. The train industry has succeeded in lowering the sound pressure level in train cars. However, the results of this study show that the diffuseness of noise has an effect on subjective annoyance. This suggests that countermeasures for aerodynamic noises can be effective for improving the acoustic characteristics within train cars.

ACKNOWLEDGMENTS

The authors thank railroad staff for their cooperation during measurements. This work was supported by a Grant-in-Aid for Young Scientists (A) from the Japan Society for the Promotion of Science (18680025, 23686086), an Ono Acoustics Research Fund, and a Sasagawa Scientific Research Grant.

REFERENCES

1. Yoshihisa, N. Fukai, M. and Yamaguchi, T., Noise levels inside subway cars in Western Europe, U.S.A. and Japan, *J. Acoust. Soc.* Jpn., 1968, 24, pp. 69-75. (in Japanese).

2. Kono, S., Sone, T. and Nimura, T., Personal reaction to daily noise exposure, *Noise Control Eng. J.*, 1982, 19, pp. 4-16.

3. Gershon, R.R.M., Neitzel, R., Barrera, M.A. and Akram, M., Pilot survey of subway and bus stop noise levels, J. *Urban Health*, 2006, 83, pp. 802-812.

4. Soeta, Y. and Shimokura, R., The impact of external environments on noise inside a train car, *Noise Control Eng. J.*, 2011, 59, pp. 581-590.

5. Hardy, A.E. Measurement and assessment of noise within passenger trains, *J. Sound Vib.*, 2000, 213, pp. 819-829.

6. Soeta, Y. and Shimokura, R., Comparison of noise characteristics in airplanes and high-speed trains, *J. Temporal Des. Arch. Environ.*, 2009, 9, pp. 22-25.

7. World Health Organization (WHO). In: Berglund, B., Lindvall, T., Schwela, D. eds. *Guidelines for Community Noise*. Geneva: World Health Organization, 1999.

8. Cohen, A., Anticaglia, J. and Jones, H., Sociocusis: hearing loss from non-occupational noise exposure, *Sound Vib.*, 1970, 4, pp. 12-20.

9. Johanning, E., Wilder, D.G., Landrigan, P.J. and Pope, M.H., Whole-body vibration exposure in subway cars and review of adverse health effect, *J. Occup. Environ. Med.*, 1991, 33, pp. pp. 605-612.

10. Chang, H.C. and Hermann, E.R., Acoustical study of a rapid train system, *Am. Ind. Hyg. Assoc. J.*, 1974, 35, pp. 640-653.

11. Remington, P.J., Wheel/rail squeal and impact noise: what do we know? What don't we know? Where do we go from here? *J. Sound Vib.*, 1987, 116, pp. 339-353.

12. van Ruiten, C.J.M, Mechanism of squeal noise generated by trams, *J. Sound Vib.*, 1988, 120, pp. 245-253.

13. Thompson, D.J. and Jones, C.J.C., A review of the modelling of wheel/rail noise generation, *J. Sound Vib.*, 2000, 231, pp. 519-536.

14. Thompson, D.J. and Jones, C.J.C., Noise and vibration from railway vehicles, in: Iwnicki, S., ed., *Handbook of Railway Vehicle Dynamics*, CRC Press, London, UK, 2006.

15. Vincenta, N., Kocha, J.R., Cholletb, H. and Guerderc, J.Y., Curve squeal of urban rolling stock-Part 1: State of the art and field measurements, *J. Sound Vib.*, 2006, 293, pp. 691-700.

16. Mellet, C., Létourneaux, F., Poisson, F. and Talotte, C., High speed train noise emission: Latest investigation of the aerodynamic/rolling noise contribution, *J. Sound Vib.*, 2006, 293, pp. 535-546.

17. Schulte-Werning, B., Beier, M., Degen, K.G. and Stiebel, D., Research on noise and vibration reduction at DB to improve the environmental friendliness of railway traffic, *J. Sound Vib.*, 2006, 293, pp. 1058-1069.

18. Nagakura, K. Localization of aerodynamic noise sources of Shinkansen trains, *J. Sound Vib.*, 2006, 293, pp. 547-556.

19. Cleon, L.M. and Williame, A., Aero-acoustic optimization of the fans and cooling circuit on SNCF's X 72500 railcar, *J. Sound Vib.*, 2000, 231, pp. 925-933.

20. Talotte, C., Gautier, P.E., Thompson, D.J. and Hanson, C., Identification, modelling and reduction potential of railway noise sources: a critical survey, *J. Sound Vib.*, 2006, 267, pp. 447-468.

21. Dittrich, M.G. and Zhang, X., The Harmonoise/IMAGINE model for traction noise of powered railway vehicles, *J. Sound Vib.*, 2006, 293, pp. 986-994.

22. Thronn, T. and Hecht, M., The sonRAIL emission model for railway noise in Switzerland, *Acta Acustica united with Acustica*, 2010, 96, pp. 873-883.

23. Forssén, J., Tober, S., Corakci, A.C., Frid, A. and Kropp, W., Modelling the interior sound field of a railway vehicle using statistical energy analysis, *Appl. Acoust.*, 2012, 73, pp. 307-311.

24. Eade, P.W. and A.E.J. Hardy, A.E.J., Railway vehicle internal noise, *J. Sound Vib.*, 1977, 57, pp. 403-415.

25. Berkhout, A. J., Vries, D.D. and Boone, M.M., A new method to acquire response in concert halls, *J. Acoust. Soc. Am.*, 1980, 68, pp. 179-183.

26. ISO 3382, *Acoustics - Measurement of the reverberation time of rooms with reference to other acoustical parameters*, International Organization for Standardization, 1997.

27. ISO 3381, *Railway applications - Acoustics-Measurement of noise inside railbound vehicle,*

SCRAP DEALER FINED FOR LOUDSPEAKER NOISE

David Bennett from Blakenall Heath, Walsall, used loudspeakers as he picked up scrap metal from streets in Cannock. Bennett was taken to court by Cannock Chase Council. He was ordered to pay a fine of £75, along with a victim surcharge of £15 and costs of £100. He admitted using a loudspeaker in the streets on August 5 last year when he appeared before Stafford Magistrates. The council's environmental health team said it regularly received complaints about the use of loudspeakers on scrap collecting vehicles. It said they caused unnecessary disturbance to residents. Councillor Janos Toth, deputy leader of the council, said. "Scrap metal dealers do provide a valuable service for people in Cannock Chase district but we receive lots of complaints from residents who are sick and tired of hearing bugles and other amplified sounds from some vehicles."